# Crystal structure, magnetic properties, x-ray-photoemission-spectroscopy, and specific-heat measurements on Pr$_2$BaO$_4$ and PrBaO$_3$

I. Felner
*Racah Institute of Physics, The Hebrew University, Jerusalem 91904, Israel*

Y. Yeshurun
*Department of Physics, Bar Ilan University, Ramat-Gan 52100, Israel*

G. Hilscher, T. Holubar, and G. Schaudy
*Institut für Experimentalphysik, Technical University of Vienna, A-1040 Vienna, Austria*

U. Yaron and O. Cohen*
*Racah Institute of Physics, The Hebrew University, Jerusalem 91904, Israel*

Y. Wolfus, E. R. Yacoby, and L. Klein
*Department of Physics, Bar Ilan University, Ramat-Gan 52100, Israel*

F. H. Potter, C. S. Rastomjee, and R. G. Egdell
*Inorganic Chemistry Laboratory, South Parks Road, Oxford OX1 3QR, United Kingdom*

We investigated Pr$_2$BaO$_4$ and PrBaO$_3$ by several complementary experimental techniques. PrBaO$_3$ crystallize in an orthorhombic structure. dc and ac susceptibility measurements exhibit irreversibility phenomena below $T_N = 11.7$ K and reveal the magnetic structure of PrBaO$_3$, which consists of an anti-ferromagnetic ordering together with a small canting of the spins which produces the ferromagnetic component. Both magnetic and specific-heat studies show that $T_N$ is not affected by the applied magnetic field up to 9 T. Pr$_2$BaO$_4$ crystallizes in an orthorhombic structure where $a = 10.56$ Å, $b = 12.43$ Å, and $c = 3.617$ Å belongs to Pnam space group. dc and ac susceptibility and specific-heat measurements show that Pr$_2$BaO$_4$ is paramagnetic down to 2 K, with a vanishing electronic specific-heat coefficient $\gamma$. X-ray photoemission spectroscopy shows that Pr is mainly trivalent in Pr$_2$BaO$_4$ and close to being tetra-valent in PrBaO$_3$. The pronounced ferromagnetic-like behavior found below 11.7 K in the Pr$_x$R$_{1-x}$Ba$_2$Cu$_3$O$_z$ system is due to the impurity of PrBaO$_3$.

## I. INTRODUCTION

Oxide superconductors have provided an unprecedented stimulus for solid state physics over the last 5 years. The search for new materials, the efforts to characterize their intrinsic physical properties and attempts to explain them, caused the rare-earth based oxides to become an important as well as interesting research area. A good example of such development in material science, particularly in characterizing new material, is given in this paper. In our extended investigation[1,2] of the superconducting and magnetic properties of the high-$T_C$ superconducting system Pr$_x$R$_{1-x}$Ba$_2$Cu$_3$O$_z$ ($R$ = rare earth), a ferromagnetic transition at 11.7 K was observed for several members of the series with higher Pr concentration. On the other hand, in a number of other compositions this transition was not found. Therefore, it was assumed that this magnetic ordering is due to an impurity phase. A further search led to the conclusion that this impurity phase exists also in Pr-Ba-O materials which do *not* contain Cu. In the Pr-Ba-O phase diagram only

PrBaO$_3$ and Pr$_2$BaO$_4$ are described as stable compounds[3] and neither has been reported as ferromagnetic at $\sim$12 K.[4] The impurity phase found in Pr$_x$R$_{1-x}$Ba$_2$Cu$_3$O$_z$ was identified as PrBaO$_3$. During the course of this work we found that several magnetic properties of this compound have already been published,[5-9] and that our present studies are qualitatively in fair agreement with the published results. A wide variety of experimental results on both PrBaO$_3$ and Pr$_2$BaO$_4$ are reported in this paper.

The crystal structure of PrBaO$_3$, where Pr ions are tetravalent by standard valence arguments, has been previously investigated by powder x-ray and neutron diffraction studies.[10] Unlike many of the transition element-based $ABO_3$ compounds, which have the cubic perovskite structure, the large Pr ion causes an ortho-rhombic distortion. The space group is Pnma, and the Pr ions reside at the center point of a distorted corner-sharing octahedron formed by six oxygen atoms as shown in Fig. 1(a). The orthorhombic distortion involves a cooperative buckling and reorientation of the octahedra with respect to each other. However, the Pr$^{4+}$ ions have

an almost octahedral arrangement of near-neighbor oxygen similar to an ideal cubic perovskite.[10] Previously, $PrBaO_3$ was studied by neutron diffraction and magnetic susceptibility[4] and no evidence was found for long-range order. However, previous magnetic susceptibility[5-8] and specific-heat measurement[7] suggested that $PrBaO_3$ orders indeed with a slight ferromagnetic component at 11.7 K; and recent high-resolution neutron powder diffraction[9] shows that the Pr spins are staggered along the $c$ axis with an averaged moment of $0.35\mu_B$. However, due to the small moment of Pr the detailed magnetic structure is not yet clear. We assume that the weak ferromagnetic-like behavior is due to the orthorhombic distortion which allows an anisotropic Dzyaloshinsky-Moriya (DM) exchange between adjacent Pr moments.

For $Pr_2BaO_4$ where the formal valency of Pr ions is three, neither crystallographic data, nor magnetic properties have been published previously. Our x-ray diffraction pattern show that this compound is also orthorhombic and isomorphous with $CaFe_2O_4$ or $Eu_3O_4$, the space group is $Pnam$ (No. 62). dc and ac magnetization measurements and specific-heat studies show clearly that $Pr_2BaO_4$ is not magnetically ordered down to 2 K. The absence of the electronic specific-heat term $\gamma$, is consistent with insulating behavior. X-ray photoemission measurements performed on both $PrBaO_3$ and $Pr_2BaO_4$, demonstrate clearly the difference between the valencies of Pr in the two compounds.

## II. EXPERIMENTAL DETAILS

$PrBaO_3$ and $Pr_2BaO_4$ were prepared by solid-state reaction of prescribed amounts of $Pr_6O_{11}$ and $BaCO_3$, which were mixed and pressed into pellets and then calcined at 950 °C in air or under oxygen atmosphere for $PrBaO_3$, and at 900 °C under hydrogen atmosphere for $Pr_2BaO_4$. The mixed powders were ground, re-pressed, sintered again under the same conditions for several times until a single phase material was achieved. The color of $Pr_2BaO_4$ is yellow, whereas the color of $PrBaO_3$ was either black or khaki. $PrBa_2Cu_3O_7$ was prepared by conventional methods.[1]

X-ray-diffraction measurements indicate that the samples are single phase and least-squares refinements of the $d$ spacing were done on the basis of an orthorhombic structure. The dc susceptibility measurements on solid ceramic pieces were carried out in a commercial SHE superconducting quantum interference device magnetometer (SQUID) in various fields as a function of temperature in the range of 4.2–300 K. All ac susceptibility measurements were carried out using a calibrated $ac$ susceptometer with ac amplitudes and frequencies ranging from 0.1 to 10 Oe and 80 Hz to 1 kHz, respectively.

Specific-heat measurements were performed over the temperature range 1.5–80 K in an automated adiabatic colorimeter employing the Nernst step heating method.

The photoemission spectra were taken at room temperature in an ESCALAB Mark II electron spectrometer equipped with 100-mm mean-radius spherical sector electron energy analyzer. The photoemission spectra were excited with Al $K_\alpha$ radiation and recorded with nominal analyzer resolution of 0.4 eV.

The well-proven technique of *in situ* oxygen/vacuum annealing[11] was used for surface preparation. In this technique, samples are clipped to a Pt stub and introduced into the preparation chamber through a fast entry lock. They are then inserted into a cooled copper coil coupled to a 1.5-KW (400 Hz) rf generator. The preparation chamber was filled with 1 bar zero grade oxygen for $PrBaO_3$ and $PrBa_2Cu_3O_7$ or left in vacuum for $Pr_2BaO_4$. A typical cleaning cycle of up to 2 h oxygen anneal at 600 °C was found effective in providing surfaces of carbon contamination with dramatically reduced levels of carbon.
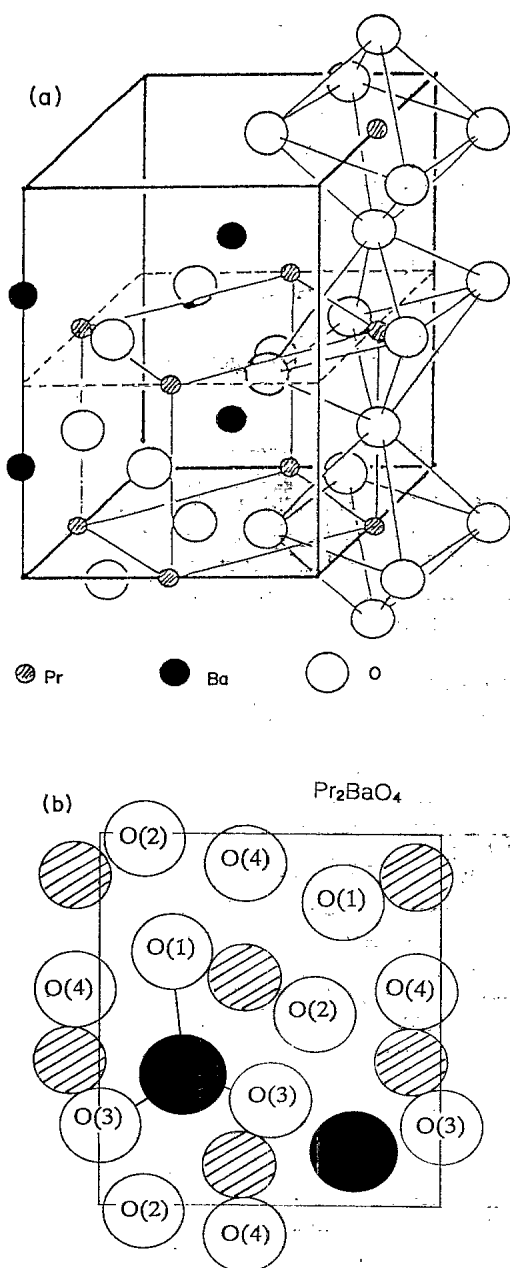


FIG. 1. (a) Orthorhombic perovskite structure of $PrBaO_3$. (b) Cross section of $Pr_2BaO_4$ structure at $z = \frac{1}{4}$.

## III. EXPERIMENTAL RESULTS AND DISCUSSION

### A. Crystal structure measurements

*$Pr_2BaO_4$.* The x-ray powder-diffraction patterns on the yellow-green $Pr_2BaO_4$ samples can be indexed on the basis of an orthorhombic structure. The lattice parameters are $a = 10.56(1)$ Å, $b = 12.48(1)$ Å, and $c = 3.617(2)$ Å in perfect agreement with the values cited by Hodorowicz *et al.*[12] Although these authors cited the lattice parameters, they did not report the space group for this material, and did not carry out the complete crystal structure analysis. Figure 2 shows the x-ray pattern of $Pr_2BaO_4$ which was taken just after preparation embracing all the $hkl$ reflections. This compound is not stable on the time scale of 3–4 months. Figure 2 shows reflections present for the following conditions: (a) $h00$, $0k0$, $00l$ only when $h,k,l = 2n$, (b) $h0l$ only when $h = 2n$, and (c) $0kl$ only when $k + l = 2n$ and (d) no regular extinctions for $hk0$ and $hkl$. These conditions are satisfied by space group $Pnam$ ($Pnma$, No. 62) and we find that the structure of $Pr_2BaO_4$ is isomorphous with $Eu_3O_4$ (Ref. 13) which is itself structurally related to calcium ferrite $CaFe_2O_4$. The relative intensity of reflections in $Pr_2BaO_4$ and $Eu_3O_4$ were found to be similar not only for the strong reflections, but also for many of the weaker reflections as well.

Both $Pr_2BaO_4$ and $Eu_3O_4$ materials contain divalent and trivalent ions and four oxygen atoms in their formula unit and the conditions mentioned above are fulfilled only by the special fourfold positions $4(c)$ in this space group. The $4(c)$ position possesses two unknown parameters namely, $x$ and $y$ where $z = \frac{1}{4}$. Each unit cell contains four formula units and all the seven atoms of $Pr_2BaO_4$ reside on two alternated planes along the short $c$ axis separated by $\frac{1}{2}c$. The data collected from our powder x-ray diffraction pattern is not sufficient to extract 14 unknown parameters, and further work will have to await suitable single crystals. Figure 1(b) exhibits the cross section of the structure at $z = \frac{1}{4}$. The assignment of $Pr^{3+}$ and $Ba^{2+}$ positions is based on the cation location of $Eu^{3+}$ an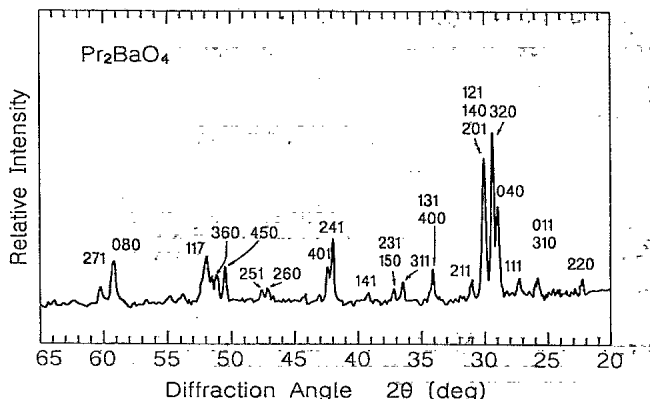d $Eu^{2+}$ in $Eu_3O_4$.[13] The coordination of oxygen around each $Pr^{3+}$ is sixfold, forming a distorted octahedron around each $Pr^{3+}$ ion [Fig. 3(a)]. Around $Ba^{2+}$ ion, the coordination is eightfold, with each Ba lying at the center of a triangular prism of six oxygen atoms; and two oxygen atoms lying out from the prism paces [Fig. 3(b)].

*$PrBaO_3$.* All the reflections observed by x-ray powder diffraction were indexed on an orthorhombic unit cell basis and indicate a single phase material. The lattice constants refined from these data are $a = 6.181$ Å, $b = 6.208$ Å, and $c = 8.727$ Å in complete agreement with Refs. 7–9. We are aware of the different assignment of the lattice parameters proposed in Ref. 9 where $a$ and $b$ are interchanged. The space group is $Pbnm$ which is the same as for $Pr_2BaO_4$. The crystal structure of $PrBaO_3$ has already been studied in great detail[10] and for the sake of clarity Fig. 1(a) exhibits its crystal structure. The almost octahedral arrangement of $Pr^{4+}$ ions in $PrBaO_3$ is quite similar to the local environment of $Pr^{3+}$ found in $Pr_2BaO_4$ Fig. 3(a). The color of $PrBaO_3$ is either black or khaki and additional oxidation at high temperatures changes the khaki sample to black. These two forms have the same lattice parameters and magnetic properties to be discussed hereafter, and are unstable on the time scale of a few months when they are stored in an ambient atmosphere. Recent neutron diffraction measurements[9] indicate that the $PrBaO_3$ samples appear to have an oxygen excess of about 2%, thus the difference in colors may be attributed to different oxygen concentration of the materials.

### B. dc and ac magnetization measurements

*$Pr_2BaO_4$.* The temperature dependence of the dc and ac susceptibilities of $Pr_2BaO_4$ has been measured at various applied fields and is presented in Fig. 4. The dc susceptibility measured at 100 Oe and 50 kOe is practically the same, which indicates that $Pr_2BaO_4$ exhibits normal paramagnetic behavior down to 4.2 K. The low field ac susceptibility is in good agreement with dc and is plotted as $1/\chi$ vs $T$ for two samples (shown in the inset). The
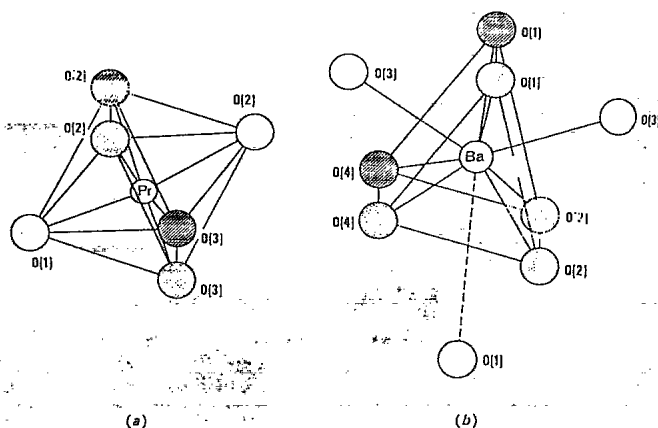


FIG. 2. X-ray diffraction pattern of the orthorhombic $Pr_2BaO_4$ with the space group $Pnam$ (No. 62).



FIG. 3. Local environment of Pr and Ba in $Pr_2BaO_4$. (a) The distorted octahedron around $Pr^{3+}$. (b) Eightfold coordination polyhedra around $Ba^{2+}$. Open circles are at the same plane $z = \frac{1}{4}$ (Fig. 1), dashed circles and strippled circles are at $z = -\frac{1}{4}$ and $z = \frac{3}{4}$, respectively.

curves of Fig. 4 adhere closely to the modified Curie-Weiss (CW) law over the entire range of the measured temperatures, and the magnetic susceptibility can be well described by the relation $\chi = \chi_0 + C/(T-\theta)$ where $\chi_0$ is the temperature independent part of the susceptibility, $C$ is the Curie constant and $\theta$ is the Curie-Weiss temperature. The least-squares fit of the dc and ac susceptibility yields an effective magnetic moment per Pr ion $P_{eff} = 2.93(\pm 0.05)\mu_\beta$ which was deduced from $C$, $\chi_0 = 1 \times 10^{-3}$ emu/mole Oe, and $\theta = -28 \pm 2$ K. The effective paramagnetic moments according to Hund's rule for $Pr^{3+}$ and $Pr^{4+}$ are 3.58 and 2.54$\mu_\beta$, respectively. The $P_{eff}$ obtained corresponds to an average valence of 3.6 for Pr in the entire temperature range. This seems to be in contradiction to simple chemical valence arguments which require $Pr^{3+}$ and with our XPS studies (see below) which show clearly that the valency of Pr is close to three. Assuming that in $Pr_2BaO_4$ Pr is indeed trivalent, a crystalline electric field (CEF) splitting of several hundreds of Kelvin, could be responsible for the reduction of $P_{eff}$. Measurements of CEF transition by inelastic neutron scattering would help to clear this point. It is worth mentioning that a similar controversy occurs for $PrBa_2Cu_3O_7$ where approximately the same $P_{eff}$ value for Pr was observed.[1] Although several experiments have been performed[14] the valency of Pr in $PrBa_2Cu_3O_7$ (either $3^+$, or $4^+$ as in a mixed valent state) is still a matter of debate. We shall address this point in the next section.

*PrBaO_3.* Previously, $PrBaO_3$ was studied by magnetic susceptibility and neutron diffraction,[4] where there was no evidence found for magnetic ordering down to 2 K. As mentioned above, recent measurements[5-9] show definitely a sharp increase of the magnetization at about $T_N = 11.7$ K which is assumed to indicate a canted antiferromagnetic structure.[6] However, a full analysis of the magnetic structure of $PrBaO_3$ has not yet been published. With the purpose of acquiring more information our magnetic measurements include the following procedures. (a) Zero-field-cooled magnetization (ZFC) was obtained by cooling the sample in nominal zero field to 5 K. Then, magnetic field was applied and the magnetization was measured during raising the temperature up to above $T_N$. (b) Next, the temperature was reduced without changing the field, and by increasing the temperature again, the field-cooled (FC) branch was obtained. (c) The sample was cooled to 5 K. The field was reduced to zero and the remanent magnetization ($M_{rem}$) was measured as a function of increasing temperature. Typical magnetization curves are displayed in Figs. 5–7.

The FC curves for $PrBaO_3$ measured for a number of applied fields are shown in Fig. 5. The shape of the curves is very suggestive of a ferromagnetic alignment occurring at $T_N = 11.7$ K. The magnetization which appears to saturate at low temperatures in low fields (100–1000 Oe), increases gradually with decreasing temperature below $T_N$ in high field (10 kOe). As can be seen, the position of $T_N$ is practically independent of H. The finding of a magnetic ordering is supported by specific-heat measurements (see later) and neutron diffraction data[9] which both indicate a magnetic transition at $T_N \sim 11.7$ K. Figure 6 shows measurements of ZFC, FC, and $M_{rem}$ at 10 Oe in which the irreversibility below $T_N$ is obvious. The ZFC branch was obtained after cooling to 6 K in "real" zero-field <0.2 Oe and the magnetization remains nearly constant up to $T_N$. The FC branch and the remanent curve coincide. Figure 7 exhibits the same magnetization curves measured at 1 kOe. The ZFC branch (the cooling field is about 2 Oe) is typically antiferromagneticlike, having a sharp peak at $T_N$ and then merges with the FC branch. The $M_{rem}$ curve has a typi-
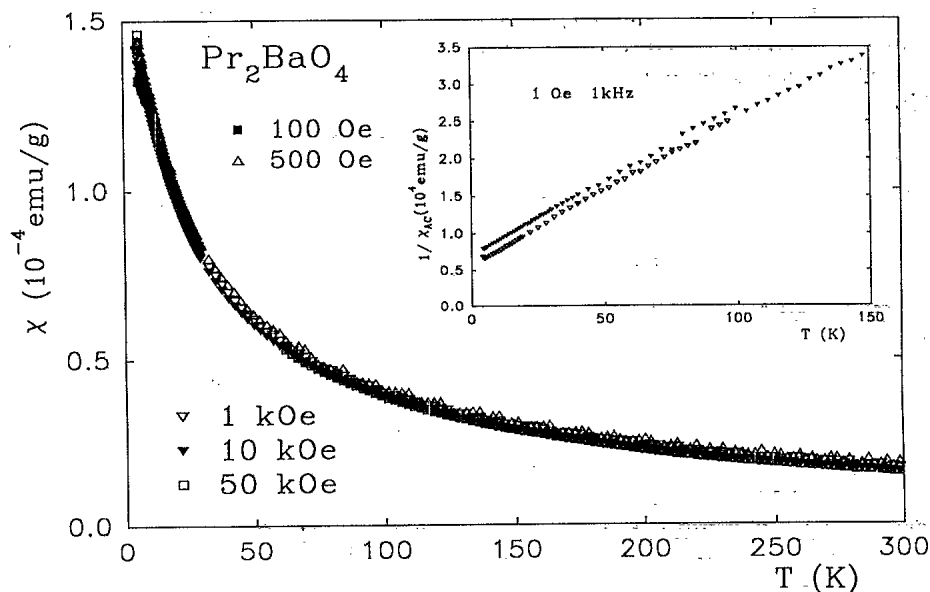


FIG. 4. Temperature dependence of the susceptibility of $Pr_2BaO_4$ at measured various fields. The inset shows $1/\chi'$ vs $T$ measured by ac susceptometer at a frequency of 1 kHz and excitation field of 1 Oe, for two different samples.
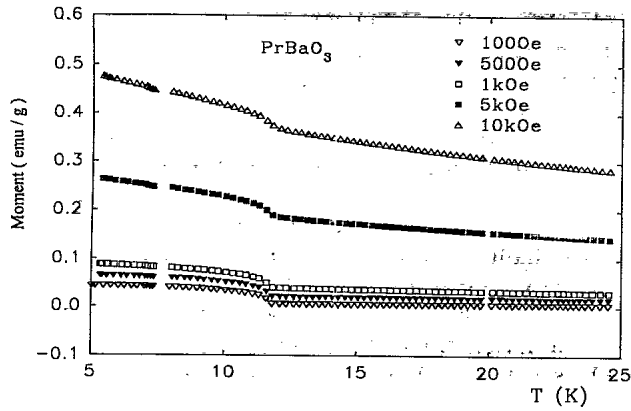
FIG. 5. Field-cooled temperature dependence of the magnetization of $PrBaO_3$ measured at various fields. Note that $T_N$ does not change with the applied field.



FIG. 7. Zero-field-cooled, field-cooled, and $M_{rem}$ magnetization curves for $PrBaO_3$ measured at 1 kOe.

cal ferromagnetic shape and becomes zero at $T_N$. Note that $M_{rem}$ is not the difference between the FC and ZFC branches.

The most informative experiments involve measurements of the remanent magnetization at constant temperature. The sample was cooled in different fields to those temperatures from above $T_N$, then the fields were turned off, and the remanent magnetization was recorded. Figure 8 displays the field dependence of $M_{rem}$ at 4.2 and 8 K. On the time scale of a few minutes there is no relaxation in $M_{rem}$.

Two features are readily observed in Fig. 8. (I) There is a rapid increase of $M_{rem}$ at low fields and $M_{rem}$ is almost saturated at few hundred Oe. The saturation values obtained at 4.2 K are $3.9 \times 10^{-3} \mu_B$ and $5 \times 10^{-3} \mu_B$ at 700 Oe and 16 kOe, respectively. Neutron diffraction[9] indicates that the Pr spins which are staggered below $T_N$ along the $c$ axis and the [110] direction possess an averaged moment of $0.35(\pm 0.05)\mu_B$ per Pr atom. This means that only a small fraction ~1% of the magnetic spins are saturated in the FC process. (II) The curve has a finite value at very low field which indicates that the remanent is easily magnetized in extremely low (~1 Oe) fields.
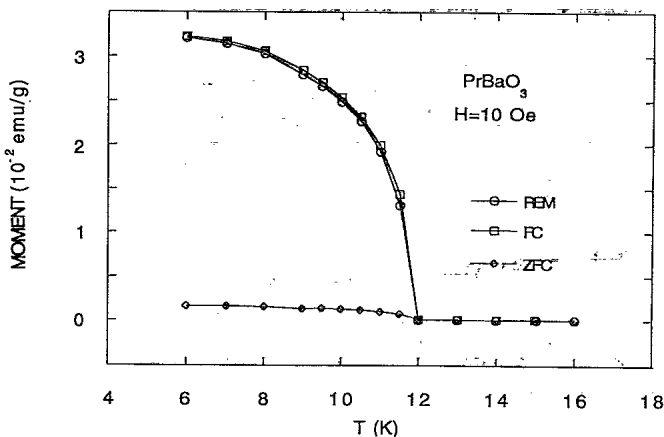
In order to study the properties of the ferromagnetic-like feature in $PrBaO_3$, the sample was cooled in fields of $H = 10$ Oe, 100 Oe, 1 kOe, and 16 kOe from above $T_N$ to 4.2 K and the hysteresis loops were measured, (Fig. 9). According to Bulman *et al.*[6] the isothermal magnetization at 4.2 K is linear up to 120 kOe and our magnetization measurements show that the curves are parallel and no magnetic moment is gained by increasing the field. A tiny hysteresis loop is opened. The difference between the curves is actually the difference between the respective remanent magnetization (see Fig. 8). The fact that the curves do not merge at high fields indicates clearly, that properties which depend on the cooling fields at $T_N$ are very stable and unchanged at low temperatures.

As a final point of interest, we have measured the real ($\chi'$) and the imaginary ($\chi''$) part of the ac susceptibility of $PrBaO_3$ between 4.2 and 30 K. A sharp maximum of $\chi'$ was found at $T_N = 11.7$ K as shown in Fig. 10. The data presented clearly indicate that the transition does not depend upon the frequency and on the rms amplitude (0.10–10 Oe, 80 Hz–1 kHz). No irreversibility phenomena is observed in FC or ZFC processes. The sharp peak which is only 0.2 K wide is not easily detectable at very small excitation fields.
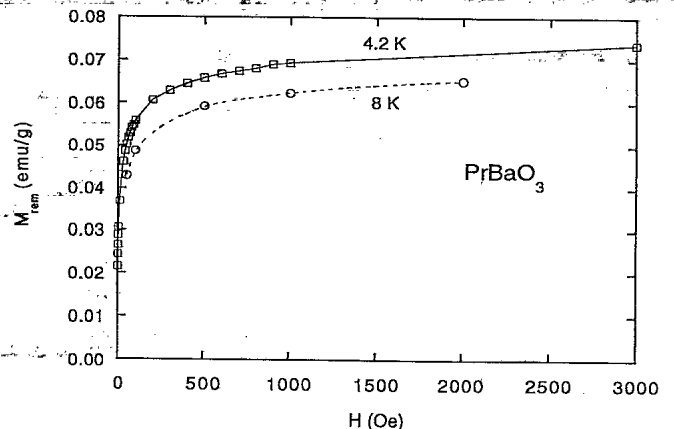


FIG. 6. Zero-field-cooled, field-cooled, and $M_{rem}$ magnetization curves for $PrBaO_3$ measured at 10 Oe.



FIG. 8. The remanent magnetization of $PrBaO_3$ measured at 4.2 and 8 K.
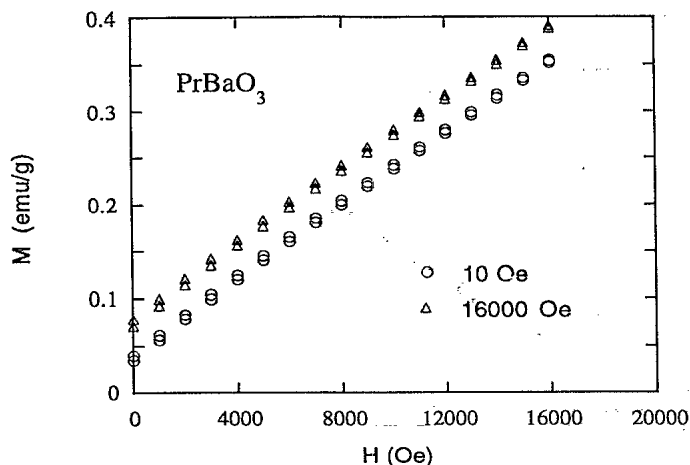
FIG. 9. Hysteresis loop of $PrBaO_3$ at 4.2 K after field-cooling process in 10 Oe and 16 kOe.

The experimental results reported here, Figs. 5–10, and the collected evidences from recent magnetic measurements[5-8] including neutron diffraction studies[9] provide an insight to the magnetic structure of $PrBaO_3$. The ZFC measurements, Figs. 5 and 6, and the ac susceptibility curve, Fig. 10, strongly support an antiferromagnetic ordering of Pr ions. The direction of the spins is not clear, and it is assumed[9] that they are staggered along the $c$ axis and the [110] direction. On the other hand the FC and $M_{rem}$, Figs. 5–9, determine a slight ferromagnetic component to the magnetic ordering. The small magnitude of the remanent magnetization ($\sim 1\%$) may imply that in the FC process the external field causes the spins to cant slightly out of their original directions. This canting abruptly aligns a component of the moments with the direction of the field and the FC curve is obtained. The pronounced irreversibility below $T_N$ and the hysteresis loops shown in Fig. 9 indicate the freezing of the canting direction. The fact that at 4.2 K the hysteresis loops are parallel and are shifted only by the remanent values shows that there is no change in the canting direction for fields up to 16 kOe.

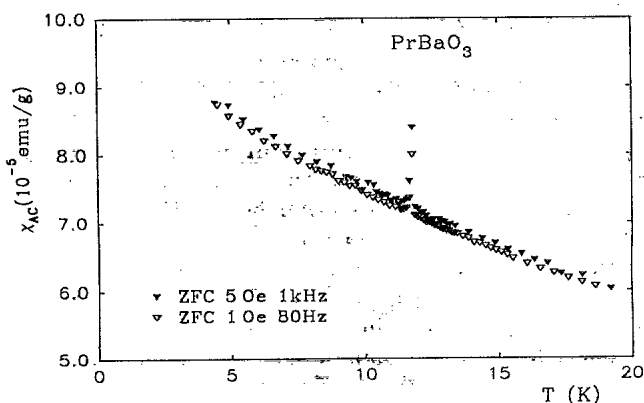The evidence of the data that both ferromagnetism and antiferromagnetism may be present in the same sample is



FIG. 10. Real part of the ac susceptibility of $PrBaO_3$ measured at frequencies of 1 kHz and rms amplitudes of 1 and 5 Oe.

consistent with the crystal structure of $PrBaO_3$ shown in Fig. 1(a). The orthorhombic distortion accompanied by tilting of nearest-neighbor $PrO_6$ octahedra, removes the inversion symmetry between the nearest-neighbor Pr sites resulting in a small off-axis ferromagnet component coexisting with the antiferromagnetic alignment of Pr moment. Similar behavior of a weak net ferromagnetic moment was observed in nearly stoichiometric single crystals of $La_2NiO_4$.[15] Such a weak ferromagnetic component is often attributed to the antisymmetric DM interactions.[16]

$PrBaO_3$ exhibits normal paramagnetic behavior above $T_N$ and adheres closely to the Curie-Weiss law over the major portion of the measured temperature. The values extracted from the susceptibility curves depend strongly on the temperature range of the fitting. A fit of CW law to $\chi$ vs $T$ curve in the range $12 < T < 25$ K yields $\chi_0 = 2.3 \times 10^{-3}$ emu/mole, $\theta = -25$ K, and an effective moment $P_{eff} = 1.6\mu_B$. A fit in the range $12 < T < 300$ K yield $P_{eff} = 2.28\mu_B$. Both values are lower than $P_{eff} = 2.58\mu_B$ obtained in Ref. 7 and smaller than expected for $Pr^{4+}$ in its $J = \frac{5}{2}$ ground state which is $2.54\mu_B$. This suppression of $P_{eff}$ suggests a significant influence of CEF on the magnetic properties at medium temperatures. It should be noted that the $P_{eff}$ values reported by various authors differ significantly from each other. The values ranging from $0.7\mu_B$ (Ref. 5) up to $3.34\mu_B$.[8]

### C. Specific-heat measurement

Because the saturation of the remanent magnetization of $PrBaO_3$, Fig. 8, is only about 1% of the averaged moment of Pr in the antiferromagnetic state, and in order to exclude the possibility that the ferromagneticlike behavior is due to an impurity phase, we have measured the specific heat $C_p$ of $PrBaO_3$ and $Pr_2BaO_4$ over the temperature range 1.5–80 K.

$Pr_2BaO_4$. The heat capacity measurements in zero field and $H = 9$ T of $Pr_2BaO_4$ presented in Fig. 11, show no signs of magnetic order above 2 K confirming the paramagnetic state derived from susceptibility measurements in Fig. 4. The usual presentation of the low temperature data in an $C/T$ versus $T^2$ plot yields a strongly downward curved graph. However a reasonably good fit to $C/T^{2/3} = A + \beta T^{3/2}$ is obtained, which means that the electronic specific heat term $\gamma$ vanishes. The inset of Fig. 11 shows the almost linear relation of $C/T^{3/2}$ against $T^{3/2}$, which is obeyed up to above 30 $K^{3/2}$. The detailed inspection of the low temperature data shows, that the tiny peak of specific heat at $H = 0$ T is shifted to lower temperatures giving rise to a significant upturn at $H = 9$ T. This anomaly can be regarded as a hint for antiferromagnetic order at about 1.5 K or lower. With respect to the negative paramagnetic $\theta$ value ($-26$ K) derived from $\chi(T)$ measurements and the above indication of a possible antiferromagnetic order, the $T^{3/2}$ term—typical for ferromagnetic spin waves—may be an accidental coincidence caused by a fairly large crystal field splitting of the low-lying levels. In this context we refer to
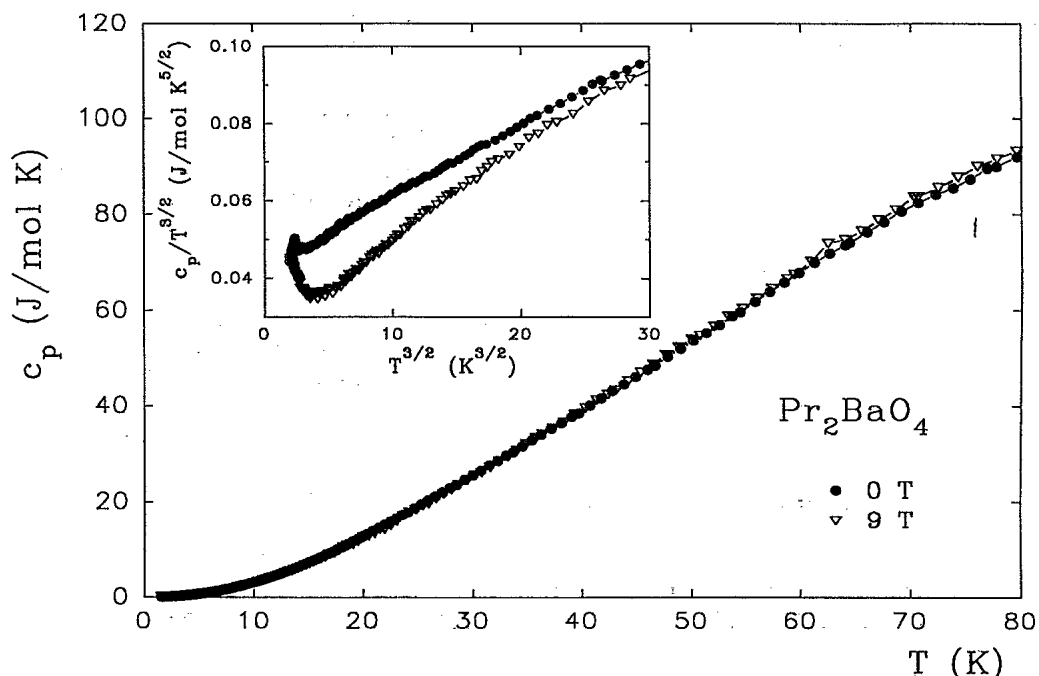
FIG. 11. Specific heat $C_p$ of $Pr_2BaO_4$ as function of temperature for external fields $H=0$ and $H=9$ T. The inset shows the $C_p/T^{3/2}$ vs $T^{3/2}$ at low temperatures.

$PrBa_2Cu_3O_7$ where the orthorhombic crystal field yields an overall splitting of about 1500 K of the $Pr^{+3}$ ground multiplet whereby the low-lying levels form a quasitriplet with a splitting of about 27 K.[17,18] If the situation in $Pr_2BaO_4$ is similar, but the splitting of the lower levels is larger; i.e., 50–100 K, the resulting crystal field contribution will be covered by the much larger lattice contribution at higher temperatures. The reduction of the 9-T specific heat data with respect to the zero field is obviously due, to a shifting of the Schottky anomaly to higher temperatures upon applying 9 T. The reduced paramagnetic moment and the slightly curved inverse susceptibility as a function of temperature support this finding.

*PrBaO$_3$.* In order to check the influence of sample preparation upon the magnetic and thermodynamic properties, we measured the heat capacity of both the black- and khaki-colored $PrBaO_3$ samples. The comparison of the data in the most sensitive regime in Fig. 12 shows that the black sample exhibits a slightly sharper anomaly at $T_N$ for both: zero field and an external field of 9 T. However, the Néel temperature of 11.7 K is the same. The overall shape of the zero-field specific-heat data are in good agreement with Refs. 6 and 7. Figure 13 demonstrates that external fields considerably broaden the sharp transition, but hardly shift the transition temperature to lower temperatures, which is in good agreement with magnetization measurements in Fig. 5. The low-temperature data show a significant upturn in the $C/T$ versus $T^2$ representation which may be indicative for a field-independent additional magnetic transition below 1.5 K. The tiny kink at about 10.5 $K^2$ might be a precursor effect and is suppressed in external fields.

We believe that this low-temperature upturn is not due to a Zeeman splitting of the ground state because of the

following arguments. According to valency counting Pr in $PrBaO_3$ is a tetravalent Kramers ion which is nicely supported by our XPS measurements. The orthorhombic symmetry removes the degeneracy of the $2F_{5/2}$ multiplet leaving $Pr^{4+}$ in a doublet ground state, whereby we presume by analogy with other rare-earth cuprates,[17,18] that the next doublet is at about 100 K or even higher. This is also consistent with the finding that up to 60 K an external field of 11 T has no significant effect upon the specific heat measurement and therefore upon the crystal field splitting up to this temperature. The molecular field of about 50 T (estimated from $T_N$) and the Pr moment of $0.34\mu_B$ determined from neutron diffraction[9] split the ground-state doublet, giving rise to a Schottky anomaly with a maximum just situated below the magnetic anomaly and can therefore not be disentangled from the magnetic contribution. Furthermore, one expects that on applying an external field the Schottky anomaly will be shifted to higher temperatures giving rise to reduction of the heat capacity at low temperatures (i.e., below the maximum of the Schottky anomaly). However, just the opposite is observed (see inset of Fig. 13). The 9-T curve is above the zero-field measurement and merges at about 9 $K^2$, which indicates that the magnon dispersion is slightly changed by the external field. We suggest that the magnon contribution varies as $\delta T^3 \exp - \Delta/kT$ where $\Delta$ is the energy of the gap in the magnon dispersion. A slight change of the gap energy by applying an external field can easily explain the change of the specific heat in external fields. In this connection we note that the magnetic contribution to the heat capacity was separated by Cao *et al.*[7] by subtracting the phonon contribution obtained from the nonmagnetic isostructural compound $ThBaO_3$. Although these authors find a clear $\delta T^3$ contri-
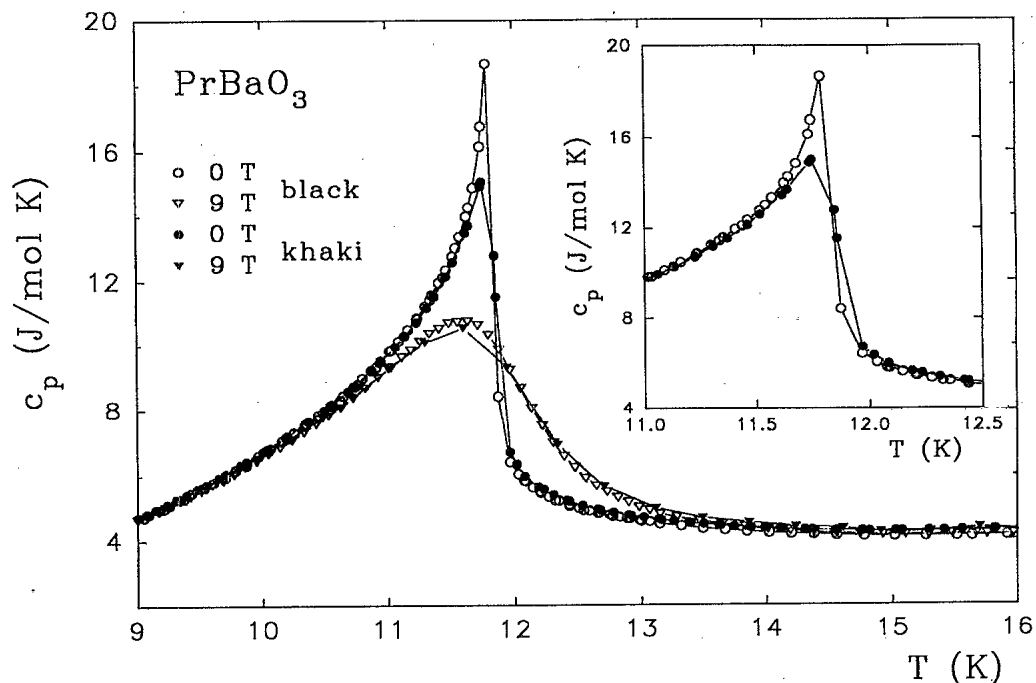
FIG. 12. Comparison of the specific heat of the black- and the khaki-colored $PrBaO_3$ in $H=0$ T and $H=9$ T. Inset: expanded view of the magnetic transition at $T_N$.

bution to the magnetic specific heat (typical for antiferromagnetic spin waves without a gap), they obtain a negative $\gamma$ value which might be due to a slight overestimation of the phonon contribution on their analysis.

The entropy associated with the magnetic transition up to 14 K accounts to 3.6 J/mol K for all measurements with and without applied field. This value is less than

$R \ln 2 = 5.67$ J/mol K expected for the doublet magnetic ground state of $Pr^{+4}$. Our value is smaller but still in reasonable agreement—since the subtraction of the unknown phonon contribution is hardly an unambiguous task—with those of Refs. 6 and 7 (4.3 and 4.0 J/mol K, respectively). The measured lower entropy may point to a slight mixed valency (but close to $Pr^{+4}$), similar to re-
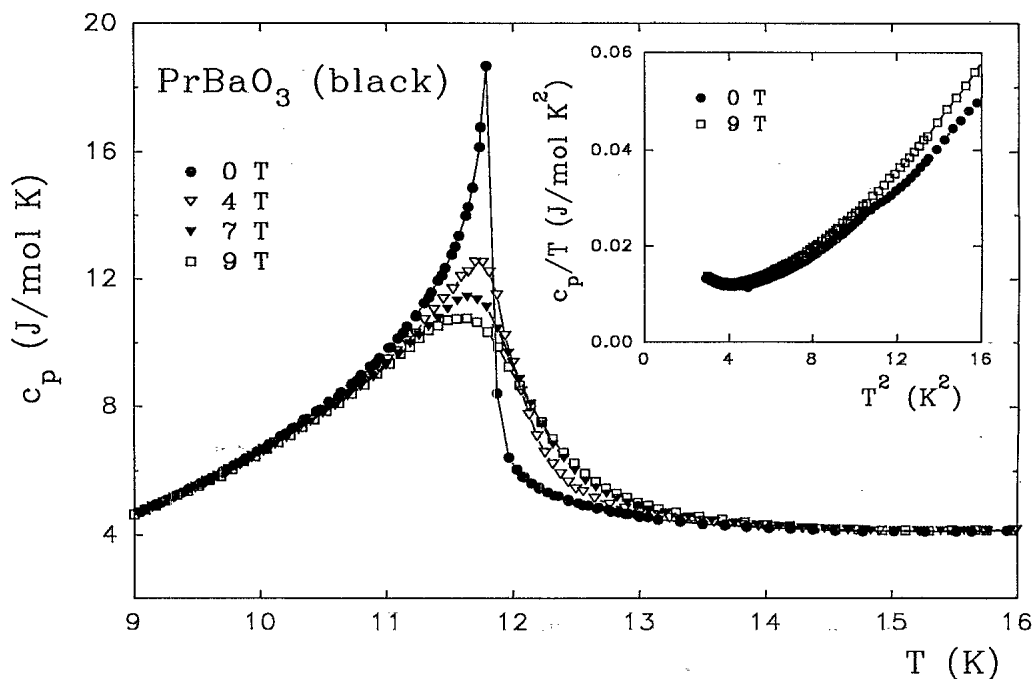


FIG. 13. Specific heat $C_p$ for $PrBaO_3$ as a function of temperature for external fields as labeled. Note that H does alter the position of the peak.

sults found for $Y_{1-x}Pr_xBa_2Cu_3O_7$ where, the valency of Pr is close to three.[17] An additional reason for the reduced entropy in $PrBaO_3$ is the entropy associated with the proposed magnetic anomaly below 1.5 K which we cannot account for in our analysis. The $\gamma = 170$–220 mJ/mol $K^2$ values were calculated by the usual procedure of extrapolating the nearly linear variation of the $C/T$ versus $T^2$ values, from above $T_N$ to $T=0$. This value is smaller than $\gamma = 400$ mJ/mol $K^2$ estimated by Bulman *et al.*[6] Such a linear term cannot be detected below $T_N$ which is in agreement with the insulating behavior of $PrBaO_3$.

The high $\chi_0$ and the finite $C/T$ value (above $T_N$) might be an artifact (in particular $\chi_0$ which implicitly describes the curvature of $1/\chi$ due to the crystal field splitting with a temperature independent Pauli susceptibility) but may be an indication for a localized heavy fermion behavior which is associated with a mixed valent character of Pr, as mentioned above.

## D. Photoemission spectroscopy measurement

Figure 14 shows Pr:$3d$ spectra of $PrBaO_3$ and of $Pr_2BaO_4$. Both samples are nonmetallic and show pronounced charging effects. Therefore the energy scales have been aligned so that the Ba:$3d_{5/2}$ binding energy, coincides with that in samples within the series $Pr_xY_{1-x}Ba_2Cu_3O_7$. Formally one can consider Pr to have valency of +4 and +3 for $PrBaO_3$ and $Pr_2BaO_4$, respectively, so that the ground-state $f$ electrons configuration can be represented as $4f^1$ and $4f^2$.

*$Pr_2BaO_4$*. The Pr$3d_{5/2}$ peak shape in $Pr_2BaO_4$ is very similar to that of $Pr_2O_3$.[19–21] The complex peak shape originates from the simultaneous effects of covalency hybridization and intraatomic electrostatic coupling be-

tween $3d$ hole and the outer unpaired $4f$ electrons.[20,21] In a detailed analysis, Ogasawara *et al.* have found recently[21] that the initial state in $Pr_2O_3$ corresponds to a relatively pure Pr:$4f^2$ configuration; in the final state though, the charge transfer energy decreases due to the existence of the core-hole potential and there is a very strong covalency mixing between oxygen and Pr ions. The final states contributing to the main peak of the Pr:$3d$, are on the average a 76%:24% mixture of $4f^2$ and $4f^3\underline{L}^1$ configurations (assign as 2 and 2′ in Fig. 14), while those of the satellite (3 and 3′) are a 24%:76% mixture [where the notation $\underline{L}^1$, etc., denotes a hole on the ligand (oxygen) atoms]. Therefore, both the Pr:$3d_{3/2}$ and Pr:$3d_{5/2}$ are splitted due to final-state configurations of $4f^3\underline{L}^1$ on the high kinetic energy side and of the dominant $4f^2\underline{L}^0$ on the low kinetic energy side.

*$PrBaO_3$*. The $PrBaO_3$ spectrum is very similar to previous published data for $PrO_2$.[22] Here the Pr formal valency is +4. In contrast to $Pr_2O_3$, the ground state must be considered as a mixture of $4f^1\underline{L}^0$ and $4f^2\underline{L}^1$ configurations ($\psi_G = a|4f^1\underline{L}^0\rangle + b|4f^2\underline{L}^1\rangle$) with initial-state $f$ electron count of around 1.6.[22] Due to final-state screening, three valence-band final states are possible, namely, $4f^1\underline{L}^0$, $4f^2\underline{L}^1$, and $4f^3\underline{L}^2$. Overall, $PrBaO_3$ ($PrO_2$) spectrum resembles that of $Pr_2BaO_4(Pr_2O_3)$ apart from two important points. (1) There is a shift of about 0.8 eV to lower kinetic energy (higher binding energy) of $PrBaO_3$ $\underline{3d}_{5/2}{}^1 4f^2\underline{L}^1$ and $3d_{5/2}{}^1 4f^3\underline{L}^2$ spectrum in respect to $Pr_2BaO_4$, which is caused by the extra (ligand) hole (Fig. 14). (2) The unscreened $\underline{3d}_{5/2}{}^1 4f^1\underline{L}^0$ peak (assigned as 1) is shifted by about 13 eV to lower kinetic energy and appears as a weak shoulder on the $\underline{3d}_{5/2}{}^1 4f^2\underline{L}^2$ peak; The unscreened $\underline{3d}_{3/2}{}^1 4f^3\underline{L}^2$ appears in the $PrBaO_3$ spectrum as a weak but distinct feature around 282 eV kinetic energy (marked as 1′). Thus, the Pr:$3d$
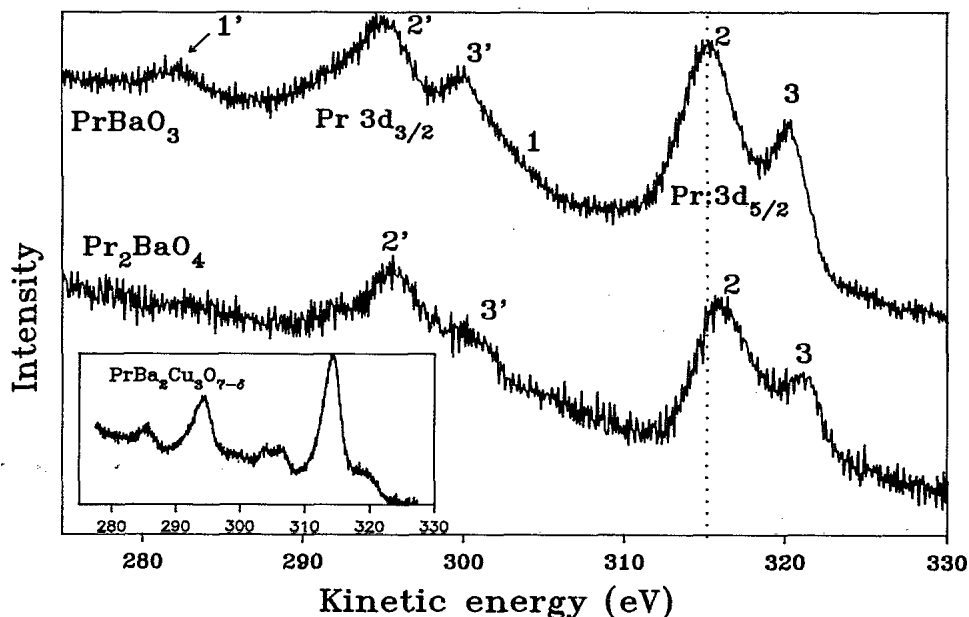


FIG. 14. X-ray photoemission spectroscopy of Pr:3d core level of $PrBaO_3$ and $Pr_2BaO_4$. The labels correspond to possible finite-state configurations explained in the text. The inset shows the Cu:$2p$/Pr:$3d$ region of $PrBa_2Cu_3O_7$.

spectrum makes it possible to distinguish between the different Pr valencies in $PrBaO_3$ (mainly $+4$) and $Pr_2BaO_4$ (mainly $+3$).

For comparison, the inset in Fig. 14 shows the Pr:$3d$ spectrum of $PrBa_2Cu_3O_7$. Unfortunately, the $3d$ structure overlaps with the Cu:$2p$ core level and the only obvious Pr:$3d$ feature is the shoulder around 320 eV. Detailed discussion of $Pr_xY_{1-x}Ba_2Cu_3O_{7-\delta}$ will be published elsewhere,[23] but it is important to notice the absence of a peak corresponding to the $\underline{3d}_{3/2}{}^14f^1\underline{L}^0$ component which would appear on the low kinetic energy side of the $\underline{Cu_2p}_{1/2}{}^1\underline{L}^03d^9$ peak, if Pr would be tetravalent in $PrBa_2Cu_3O_7$.

## IV. CONCLUDING REMARKS

We report at the first on crystallographic and magnetic properties of $Pr_2BaO_4$, which crystallizes in an orthorhombic structure belongs to space group *Pnam*. $Pr_2BaO_4$ is paramagnetic down to 2 K. $\gamma = 0$ was deducted from specific-heat measurements. The valency of Pr might be considered controversial, as in $PrBa_2Cu_3O_7$, if only the reduced effective $P_{\text{eff}} = 2.93\mu_B$ moment is considered which would correspond to an effective average valency of 3.6 in $Pr_2BaO_4$. On the other hand XPS studies indicate that Pr is mainly in a trivalent state. In that respect, $Pr_2BaO_4$ resembles $PrBa_2Cu_3O_7$. However, specific-heat measurements support in both systems that crystal field effects seems to be the main reason for the reduction of the effective paramagnetic moment.

$PrBaO_3$ orders antiferromagnetically with a weak ferromagnetic component at $T_N = 11.7$ K. Neither the applied dc fields up to 9 T nor the frequency of ac field affect $T_N$. The irreversibility below $T_N$ is attributed to slight canting of Pr spins during the FC process which produces the ferromagneticlike component, which account to $\sim 1\%$ of Pr moment. This canted magnetic structure is a result of the distorted orthorhombic perovskite structure of $PrBaO_3$ which allows an anisotropy Dzyaloshinsky-Moriya exchange between adjacent Pr moments. The entropy associated with the magnetic transition 3.6 J/mol K which is less than $R \ln2$ expected for a doublet magnetic ground state of $Pr^{4+}$, points to a slight mixed valent state in $PrBaO_3$. The high $\gamma = 200$ mJ/mol K$^2$ is typical for localized heavy fermion system.

The pronounced ferromagnetic behavior found in $Pr_xR_{1-x}Ba_2Cu_3O_z$ system is due to $PrBaO_3$. It means that under standard synthesis conditions of bulk ceramics, the formation of $PrBaO_3$ competes with the formation of the $YBa_2Cu_3O_7$ type structure.

*Present address: Centre for High Temperature Superconductivity, Imperial College, London SW7, United Kingdom.

[1] I. Felner *et al.*, Phys. Rev. B **40**, 6739 (1989).

[2] G. Wortmann and I. Felner, Solid State Commun. **75**, 981 (1990).

[3] *Handbook on Physics and Chemistry of Rare-Earth*, edited by K. A. Geschneidner, Jr. and C. Eyring (North-Holland, Amsterdam, 1980), Vol. 3, p. 337.

[4] B. C. Tofield, A. J. Jacobson, and B. E. F. Fender, J. Phys. C **5**, 2887 (1972).

[5] M. Bickel, G. L. Goodman, L. Soderholm, and B. Kanellakopulos, J. Solid State Chem. **76**, 178 (1988).

[6] J. B. Bulman *et al.*, J. Appl. Phys. **69**, 4874 (1991).

[7] G. Cao *et al.*, J. Appl. Phys. **70**, 6332 (1991).

[8] B. Lippold *et al.*, Solid State Commun. **79**, 487 (1991).

[9] N. Rosov *et al.*, Phys. Rev. B **45**, 982 (1992).

[10] A. J. Jacobson, B. C. Tofield, and B. E. F. Fender, Acta Crystallogr. Sect. B **28**, 956 (1972).

[11] W. R. Flavell and R. G. Egdell, Supercond. Sci. Technol. **1**, 118 (1988).

[12] S. A. Hodorowicz, J. Czerwonka, and H. A. Eick, J. Solid State Chem. **88**, 391 (1990).

[13] R. C. Rau, Acta Crystallogr. Sect. B **20**, 716 (1966).

[14] S. Ghamoty *et al.*, Acta Crystallogr. **43**, 5430 (1991).

[15] D. J. Buttrey, J. M. Honig, and C. N. R. Rao, J. Solid State Chem. **64**, 287 (1986).

[16] T. Thio *et al.*, Phys. Rev. B **38**, 905 (1988).

[17] T. Holubar, G. Schaudy, N. Pillmayr, G. Hilscher, M. Divis, and V. Nekvasil, J. Magn. Magn. Mater. **104-107**, 479 (1992).

[18] V. Nekvasil, J. Phys. (Paris) Colloq. **43**, C8-2177 (1988).

[19] P. Burroughs, A. Hammett, A. F. Orchard, and G. Thornton, J. Chem. Soc. Dalton Trans. **17**, 1686 (1976).

[20] A. F. Orchard and G. Thornton, J. Electron. Spectrosc. **13**, 27 (1978).

[21] H. Ogasawara, A. Kotani, R. Potze, G. A. Sawatzky, and B. T. Thole, Phys. Rev. B **44**, 5465 (1991).

[22] A. Bianconi, A. Kotani, K. Okada, R. Giorgi, A. Granado, and T. Miyahara, Phys. Rev. B **38**, 3433 (1988).

[23] O. Cohen, F.H. Potter, C. S. Rastomjee, and R. G. Egdell (unpublished).